Detecting absolute human knee angle and angular velocity using accelerometers and rate gyroscopes

R. Williamson[1] B. J. Andrews[2]

[1]Second Sight, LLC, Stanford, California, USA
[2]National Spinal Injuries Center at the Stoke Mandeville Hospital and the Department of Cybernetics, University of Reading, UK

Abstract—*Knee joint angle and angular velocity were calculated in real time during standing up and sitting down. Two small modules comprising rate gyroscopes and accelerometers were attached to the thigh and shank of two able-bodied volunteers and one T_5 ASIA(A) paraplegic assisted by functional electrical stimulation (FES). The offset and drift of the rate gyroscopes was compensated for by auto-resetting and auto-nulling algorithms. The tilt of the limb segments was calculated by combining the signals of the accelerometer and the rate gyroscope. The joint angle was calculated as the difference in tilt of the segments. The modules were also tested on a two-dimensional model. The mean differences between the rate gyroscope–accelerometer system and the reference goniometer for the model, able-bodied and paraplegic standing trials were 2.1°, 2.4° and 2.3° respectively for knee angle and 2.3° s^{-1}, 5.0° s^{-1} and 11.8° s^{-1} respectively for knee velocity. The rate gyroscope–accelerometer system was more accurate than using the accelerometer as a tilt meter, possibly due to the greater bandwidth of the rate gyroscope–accelerometer system.*

Keywords—*Gait analysis, FES, Accelerometer, Rate gyroscope, Goniometer, Motion sensors*

Med. Biol. Eng. Comput., 2001, **39**, 1–9

1 Introduction

MANY CLOSED loop control systems in functional electrical stimulation (FES) systems proposed to improve standing and walking have been based on sensing knee joint angle and angular velocity (PETROFSKY *et al.*, 1984; ANDREWS *et al.*, 1989; MULDER *et al.*, 1992; CRAGO *et al.*, 1996). Of the sensors and measurement systems that exist for studying human motion, few are candidates for routine FES use outside the laboratory (CRAGO *et al.*, 1986). A sensor frequently used for FES in laboratory demonstrations is the Biometrics (formally Penny and Giles) flexible goniometer.* CRAGO *et al.* (1986) noted that during sit-to-stand trials, this type of goniometer needed to be calibrated for each trial due to slipping with use. Our experience repeated this finding, and additionally indicated that this device's fragile nature and high current consumption could limit its application to everyday FES systems. The goniometer measures the angle perpendicular to the plane of its orientation. This plane can be difficult or impossible to accurately align perpendicular to the knee joint axis, and hence the estimate of knee angle from the goniometer could be inaccurate. If angular velocity is used as a control variable, techniques for numerical differentiation of the goniometer signal could amplify the high frequency noise components.

Rate gyroscopes offer an alternative method for monitoring human joint rotations. Previously, real-time detection of angles based on rate gyroscopes was limited due to the zero frequency offset when stationary (MURATA trade literature, 1999). MIYAZAKI (1997) integrated a 0.5 Hz high-pass filtered piezoelectric rate gyroscope attached to the leg and determined hip flexion extension angle and walking speed. KATARIA and ABBAS (1998) estimated angles from an integrated signal of a 0.0047 Hz high-pass filtered rate gyroscope. In both of these reports, the motions examined were cyclical with periods of the order of a second, hence a zero frequency component of angular velocity was expected to have a zero value. For non-cyclical motions, such as standing-up, the application of this technique might be inappropriate.

LUINGE *et al.* (1999) continued the tradition of using accelerometery to detect motion (SMIDT *et al.*, 1971; MORRIS, 1973; SMIDT *et al.*, 1977; WILLEMSEN *et al.*, 1991; HEYN *et al.*, 1996). He proposed predicting errors using a Kalman filter and the segmental tilt from accelerometers, and compensated for these errors using a feedback loop. In their computer simulations, errors in excess of 5° were produced.

In this paper the signal from the rate gyroscope was integrated to produce an estimate of angle. Accelerometers were used to compensate for slowly occurring errors in the integral of the rate gyroscope. The combinations of two error correcting (auto-resetting) and three offset correcting (auto-nulling) techniques were explored, and compared to the real-time signal acquisition accuracy of the goniometer and accelerometer based estimates of knee angle and angular velocity. As a potential

* Biometrics Ltd., 1999.

Correspondence should be addressed to Dr B. J. Andrews; email: brianandrews55@hotmail.com

First received 4 April 2000 and in final form 26 March 2001

MBEC online number: 20013589

application of this sensing technique is in FES systems, the robustness of the system with respect to FES induced noise was a concern and tested.

One extension of this technique has previously been described as a Gyrogoniometer (ANDREWS and WILLIAMSON, 1997).

2 Theory of operation

2.1 *Determination of angle and angular velocity*

In Fig. 1, the accelerometer signals are α_x and α_y, and the rate gyroscope signal is ω. The zero frequency component, or null or offset, of the rate gyroscope is ω_0.

The sensors are placed on the individual when he or she is at rest. At the start of a trial, a computer program calculates the tilt of a segment using the accelerometer measurements sampled at 100 Hz. The arctangent function is used to calculate the angle. This function is real for an infinite range of inputs, and is less sensitive to noise, which are two advantages in comparison to the arcsine.

$$\left(\frac{d}{da_y}\tan^{-1}(a_y/a_x)\right)^2 + \left(\frac{d}{da_x}\tan^{-1}(a_y/a_x)\right)^2$$
$$= 1 < \frac{1}{1-a_y^2} = \left(\frac{d}{da_y}(\sin^{-1}(a_y))\right)^2 \;|||(a_x, a_y < 1) \quad (1)$$

The initial estimation of the angle is calculated by averaging the angle from the accelerometers over 50 samples (k):

$$\theta_n(0) = \sum_{k=0}^{49} \tan^{-1}(a_{y,n}(k)/a_{x,n}(k))/50 \quad (2)$$

The zero frequency offset of the rate gyroscope is determined from

$$\omega_n(0) = \sum_{k=0}^{49} \omega_n(k)/50 \quad (3)$$

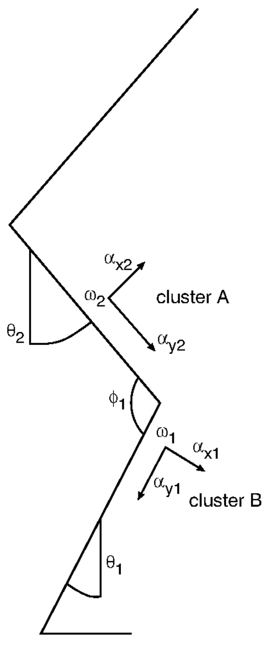

Fig. 1 *Determination of knee angle from accelerometers and rate gyroscopes. Accelerometers α_{x1}, α_{y1} and rate gyroscope ω_1 are placed on the shank in the sagittal plane. The tilt of the shank, θ_1, is calculated from this cluster. Accelerometers α_{x2}, α_{y2} and rate gyroscope ω_2 are placed on the thigh in the sagittal plane. The tilt of the thigh, θ_2, is calculated from this cluster. The knee angle, ϕ_1, is the difference in tilts of the two segments.*

After this time ($k > 49$), the tilt of the segment can be calculated by digitally integrating the signal from the rate gyroscope:

$$\theta_n(k+1) = (\omega_n(k+1) - \omega_n(0)) \cdot \Delta t + \theta_n(k) \quad (4)$$

The angle across the joint can be calculated as

$$\phi_n = \theta_{n+1} - \theta_n \quad (5)$$

2.2 *Auto-nulling the rate gyroscopes and auto-resetting the integrators*

The null of the rate gyroscope must be calculated when the rate gyroscope is stationary. Accelerometers were used to detect when the rate gyroscope was stationary. When low variance of the accelerometer signal was present, automatic nulling occurred, i.e.

If

$$\sqrt{\frac{\sum_{k-45}^{k} \theta(k)^2_{accel}\Delta t - \left(\sum_{k-45}^{k} \theta(k)_{accel}\Delta t\right)^2}{45}} < \sigma \quad (6)$$

then

$$\omega_0 = \sum_{k-45}^{k} \omega(k)/45 \quad (7)$$

σ was set at 0.1°. This variance was calculated every 0.1 s, or ten samples.

An error in the integral of the rate gyroscope can exist due to an incorrect null. Low-pass filtered accelerometers should provide an accurate estimate of the tilt of a segment, although delayed in time. A similarly delayed-in-time integral of the rate gyroscope was checked against the accelerometers' calculation of tilt, i.e.

If

$$\frac{\left|\sum_{k-30}^{k} \theta_{r.gyro}(k-gd) - \theta_{accel}(k)\right|}{30} > \lambda \quad (8)$$

then

$$\theta_{r.gyro}(k) = \theta_{r.gyro}(k) - \frac{\sum_{k-30}^{k} \theta_{r.gyro}(k-gd) - \theta_{accel}(k)}{30} \quad (9)$$

where gd is the group delay of the low-pass filter applied to the accelerometers.

This rule was evaluated every 0.1 s, with the threshold λ set at 1°. In these trials, the accelerometers were based on a fourth-order Butterworth filter of 2.5 Hz, $gd = 16$.

For sit to stand to sit trials, nulling and resetting intervals of 0.45 s should be easily obtained. If these techniques were applied to a gait analysis system, the sampling rate could be increased to achieve both a population (in this case 30 points) and an interval of stationarity.

3 Methods

3.1 *Data acquisition*

The accelerometers* were calibrated at ± 1 g levels before the trials. Each cluster was set in position for 2.56 s and sampled at 100 Hz. The ambient temperature of the room was 21 °C, and on the days of the trial varied between 20 and 21 °C. The variation in DC baseline of the accelerometers for a temperature variation

* ADXL202JQC, Analog Devices.

of 1 °C was 6 mV, or 0.4° and was within specifications for the devices. The linearity of the accelerometers was $<0.5\%$, as suggested in the specification, and confirmed prior to these trials. The frequency response had a 3 dB corner at 1.02 kHz, and the linear range of the device was ± 2 g.

The sensitivity of the rate gyroscope was specified as 1.1 mV/(°/s), and was not calibrated (ENC05GA, MURATA, 1999). The range of the rate gyroscope was $100°\,s^{-1}$ and the frequency response was not specified. The accelerometer signals were amplified† to provide a 3 V range for accelerations between ± 1 g and single-stage low-pass filtered at 16 Hz.

A serial 12 bit A/D converter‡ with a range of 4.096 V was controlled via a queued peripheral serial interface (QSPI) bus mastered by an Onset Computers model TT8 – MC68332-based microcontroller with a 2 MB removable microdisk flash memory.** The Persistor™ was used to store the data samples of the accelerometers and rate gyroscope signals at a frequency of 100 Hz.

The reference device, a Biometrics M180 goniometer was powered by a ± 2.5 V supply, amplified†† and input directly to a 12 bit A/D channel of the PC‡‡. This A/D converter was controlled by NI's LabWindows/CVI 5.0.1 software. A synchronisation signal from the TT8 was sampled with the goniometer to co-ordinate the sampling of the goniometer to that of the accelerometer and rate gyroscope clusters. For the tests on the able bodied and paraplegic subject, the goniometer signal was sampled and stored with the accelerometer and rate gyroscope signals. The goniometer output was filtered with a second-order, low-pass Butterworth filter. The signal was then reversed in time and filtered, i.e. anticasually, to cancel phase distortions. The 3 dB corner frequency was set at 2.5 Hz and the filtering process implemented using MATLAB v 5.2.1. To obtain angular velocity, the low-pass filtered goniometer signal was differentiated using the simple difference formulae:

$$\dot{\theta}(t) = \theta(t) - \theta(t-1)/\Delta t \tag{10}$$

3.2 *Combination of the rate gyroscope and accelerometers*

Two modules comprised of accelerometers and rate gyroscopes were attached to the thigh and shank. Each cluster used one rate gyroscope and one 2D accelerometer. The cluster dimensions were $5 \times 3 \times 1.7$ cm, and weight 85 g, and are indicated in subsequent figures. Thigh and shank inclinations were calculated using eqn 4 and the knee angle using eqn 5. Knee angular velocity was computed using eqn 10.

Three nulling techniques and two resetting techniques were tested. These are referred to alphabetically as methods A–F.

A. The rate gyroscope was nulled 24 h before the trial and the integrator was not reset during the trial.
B. The rate gyroscope was nulled once at the beginning of each trial and the integrator was not reset during the trial.
C. The rate gyroscope was nulled automatically in accordance with eqns. 6 and 7; the integrator was not reset during the trial.
D. The rate gyroscope was nulled 24 h prior to the trial, and the integrator was reset in accordance with eqns 8 and 9.
E. The rate gyroscope was nulled at the beginning of each trial and the integrator was reset in accordance with eqns 8 and 9.
F. The rate gyroscope was nulled automatically in accordance with eqns 6 and 7 and reset in accordance with eqns 8 and 9.

† Analog devices AMP04FNZ6642.
‡ Maxim Max186.
** CF8 Persistor™, supplied by Peripheral Issues Inc.
†† Analog devices AMP04FNZ6642.
‡‡ National Instruments AT-MIO-16L card.

The accuracy of each method was computed and compared in pairs for the trials. If a method was found to be significantly less accurate than the other methods, or if it produced errors that could be difficult to use in a controller, the method was disregarded from further testing.

For a means of comparison, the knee angle and angular velocity were calculated by the accelerometers. The signal from the accelerometers was low-pass filtered in attempts to lower the RMS difference between the angle calculated by the accelerometers and the reference signal. The low-pass filter was a digital implementation of a second-order digital Butterworth. The 3 dB corner frequencies of the filter were varied.

A second estimation of knee angle and angular velocity was derived from the goniometer as a means of comparison with the combined accelerometer–rate gyroscope system. Knee angle and angular velocity were calculated in real time through evaluating the RMS difference between the reference signal, which is filtered causally and anticausally, to a signal that was left unfiltered or filtered causally.

Paired t tests with an alpha of 0.01 were used to compare pairs of methods.

3.3 *Single and multi-segment tests on the two-dimensional model*

The two sensor clusters and the electrogoniometer were arranged as depicted in Fig. 2 for single segment tilt measurements. The model was aligned in the vertical plane. The sensor clusters, A and B, were mounted on the upper segment of the 2-D model; the goniometer was set across the joint of the

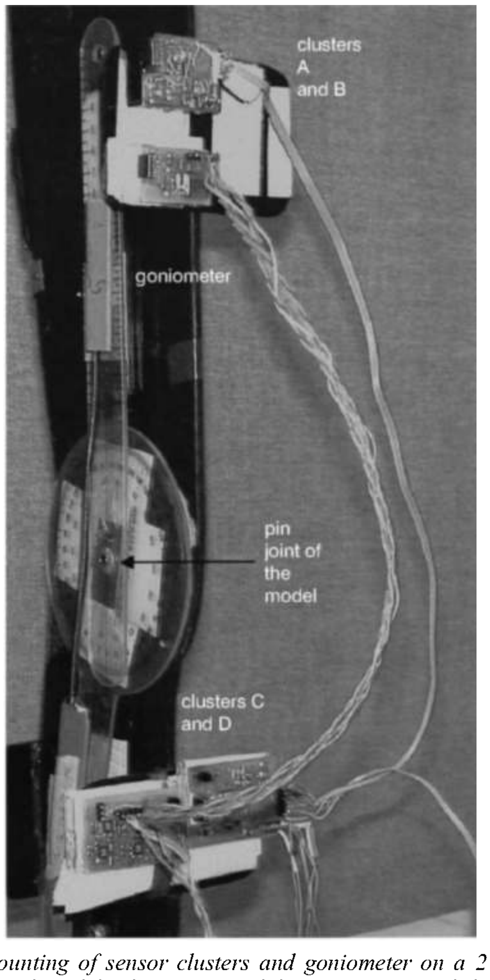

Fig. 2 *Mounting of sensor clusters and goniometer on a 2 dimensional model. The position of the goniometer and the sensor clusters are indicated. The model rotates about a single pin joint. This constrains the motion to 2 dimensions.*

model. The upper segment of the model was moved through a range of motion of approximately 95° in a single sweep in approximately 2 s. An additional 2 s of data were recorded at the beginning and the end of each trial. Tilt and rate of change of tilt were calculated for methods A–F, and from low-pass filtering of only the accelerometer signals using eqn 1 for eight separate recordings.

In the multi-segment tests, the sensor clusters A and B were positioned on the upper segment of the model. Clusters C and D were positioned on the lower segment. The goniometer was again placed across the joint of the model. In this trial, both segments of the model were moved manually to simulate sit to stand and stand to sit manoeuvres. The manoeuvres were repeated six times.

3.4 *Sit–stand–sit trials*

Repeated sit-to-stand and stand-to-sit manoeuvres were performed by one able-bodied female (age 23, height 170 cm, weight 52 kg), and one able-bodied male (age 27, height 190 cm, weight 80 kg). The electrogoniometers were attached using double sided tape across both knees to provide a reference for knee joint angle for the bilateral recordings. The female performed 18 and the male eight sit-stand-sit manoeuvres.

The simple calibration of the goniometer by recording its averaged output with the knee in 180° and 90° extension as observed with a plastic protractor was found to be inadequate. In previous trials, the average knee extension, as recorded by the electrogoniometer while standing was observed to vary between 165° and 190°, and 70° and 120° while sitting, possibly due to slipping of the goniometer with respect to the skin. For these trials, the electrogoniometer was calibrated to a physical goniometer during a 0.5 s interval when the subject was sitting prior to standing up and during standing during standing.

The sensor clusters and Biometrics goniometer were also attached to the right leg of a male paraplegic [28 years, 7 years post injury, 180 cm, 78 kg, T-5 ASIA(A)]. This individual was skilled in the use of a simple two-channel surface electrode FES system operationally similar to that described by KRALJ and BAJD (1989). Self-adhesive hydrogel electrodes of dimensions 1″ × 3″ were placed approximately over the motor points of the vastus lateralis and rectus femoris. Reference electrodes were placed on the front of the thigh, approximately 8 cm above the knee. The goniometer was attached laterally, as shown in Fig. 3. The right shank sensor clusters were mounted onto ankle foot orthoses. The right upper cluster was fixed to the reference electrodes. The subject completed a total of eight standing up trials assisted by FES in one clinical laboratory session. Knee angle and angular velocity were computed as they were in the able bodied tests.

3.5 *Influence of FES*

FES could lower the precision of a sensor system by adding high frequency noise to the system that does not represent movements about the joint through

(1) muscle vibrations transmitted through the skin (25 Hz),
(2) induced electrical interference in the sensor interface circuitry and interconnecting cables due to the FES (200 V, 200 μs pulses repeated at 25 Hz).

To examine these artifacts, quiet standing tests were conducted with and without FES. Quiet standing with FES and without FES was supported by an anterior floor reaction orthosis (ANDREWS *et al.*, 1989), shown in Fig. 3.

The individual was standing with fully extended knees, and the knee could not be seen to move. From this observation, it was assumed that only low frequency components (< 1 Hz) should exist in the signal. The increased RMS of the high frequency components of the knee angle should indicate a lessened level of precision.

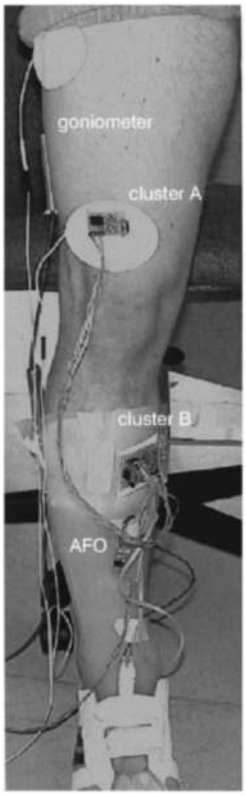

Fig. 3 *Paraplegic volunteer wearing sensor clusters, AFO, goniometer and stimulating electrodes. Sensor cluster B was mounted on the AFO as indicated in the figure. The goniometer was attached as indicated in the trade literature. The active FES electrode was placed near the motor point of the vastus lateralis. The reference electrode was placed above the knee. Sensor cluster A was mounted on the top of this electrode.*

The signals were digitally low-pass filters with typical 3 dB corner frequencies of 2.5, 5 and 10 Hz. The bandwidth and high frequency components were further reduced by filtering causally and anticausally with a second-order digital Butterworth filter with 3 dB cutoff 2.5 Hz, attenuating the 20 Hz pick up by an additional 78 dB. The residual signal was calculated by subtraction of the original low-pass filtered signal from the reduced bandwidth signal. The residual signal contained high frequency components that were not removed by the original filtering technique.

4 Results

4.1 *Dynamic single and multi-segment inclination test*

Table 1 summarises the results of the single segment test. Individual calculations were made from the same data set for methods A–F as described above.

The integrated rate gyroscope signals nulled on a previous day, methods A and D, were not as accurate as B, C, E, or F. For this reason, methods A and D were disregarded from further testing. Methods B, C, E, and F were not statistically different.

Tilt and rate of change of tilt were also calculated by the accelerometers and by the electrogoniometer. Table 2 lists the results for different cutoff frequencies of the second-order Butterworth filters applied to the accelerometers and goniometer.

The most accurate calculation of tilt from the accelerometers was computed without additional digital filtering, and was used as the accelerometer measurement in further trials. This calcula-

Table 1 Errors [mean and (standard deviation)] of estimates of tilt and rate of change of tilt by the resetting and nulling methods. The results were averaged over eight trials conducted through moving only the upper segment of the model

	Tilt (°)						
Integrator reset? Method for null Method	No Prev. day A	No Start of trial B	No Auto C	Auto Prev. day D	Auto Start of trial E	Auto Auto F	Rate of change of tilt (°/s)
Cluster A mean	28 (5)	0.7 (0.3)	0.7 (0.2)	7 (2)	0.7 (0.3)	0.8 (0.2)	2.9 (0.3)
Cluster B mean	53 (9)	2.1 (0.8)	1.1 (0.4)	13 (5)	1.2 (0.2)	0.8 (0.2)	2.8 (0.3)

Table 2 Errors [mean and (standard deviation)] of tilt and rate of change of tilt as calculated by the accelerometer and the goniometer for movement of the upper segment of the model. The RMS error was calculated between each signal and the filtered or unfiltered accelerometer or goniometer signal reference goniometer

	Tilt (°)					
	Unfiltered	10 Hz	5 Hz	2.5 Hz	1.5 Hz	1 Hz
Accel 1	2.3 (0.7)	2.5 (0.6)	3.0 (0.8)	4.6 (1.1)	7.1 (1.6)	10.3 (2.2)
Accel 2	2.5 (0.7)	2.7 (0.7)	3.2 (0.8)	4.8 (1.1)	7.3 (1.6)	10.5 (2.2)
Gonio	0.11 (0.02)	0.95 (0.18)	2.0 (0.4)	3.9 (0.8)	6.6 (1.2)	9.9 (1.9)
	Angular velocity					
Accel 1	42 (9)	24 (5)	18 (4)	20 (4)	25 (6)	93 (20)
Accel 2	44 (10)	24 (5)	17 (4)	20 (5)	26 (5)	74 (15)
Gonio	9 (2)	11 (3)	14 (3)	18 (4)	23 (6)	28 (7)

tion of tilt was less accurate than any of methods B, C, D, and F. The rate gyroscope calculated rate of change of tilt more accurately than the differentiated goniometer or the differentiated accelerometers.

Although digital filtering lowered the high frequency noise components, it also lowered the bandwidth and response time of the system. This decrease in response time caused an increase in the errors calculated in Table 2.

An example recording from the multi-segment tests is shown in Fig. 4. Table 3 summarises the results.

Auto-resetting of the integral of the rate gyroscope occurred at the discontinuities, indicated by arrows, at times 2.8, 3.8, 4.8,

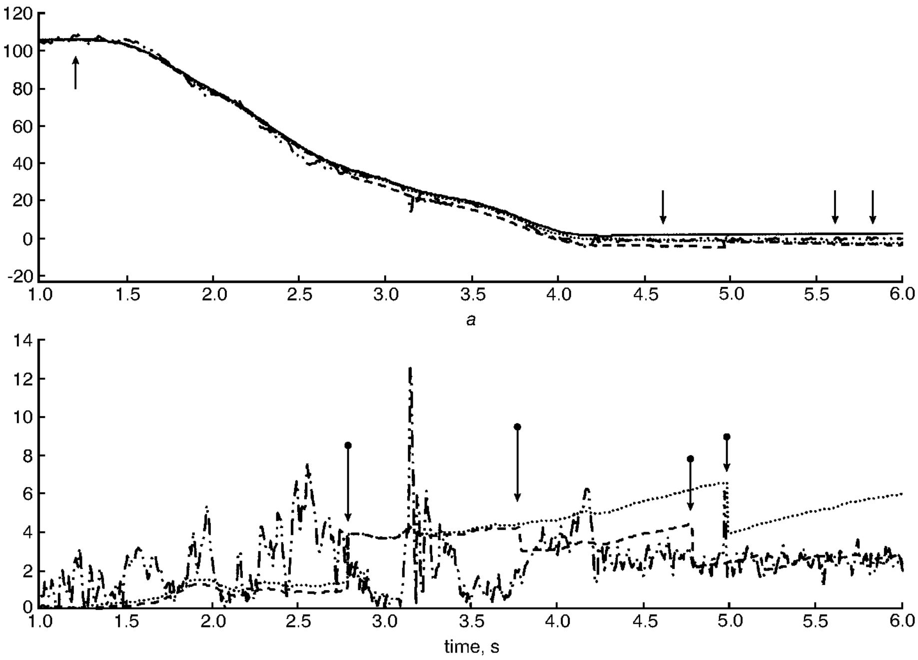

Fig. 4 *Angle calculated by goniometers, accelerometers and rate gyroscopes on the two dimensional model. The goniometer is the solid trace. The accelerometer is the long dashed and dotted line; Method E, resetting the integral of the rate gyroscope without auto-nulling the rate gyroscope, is displayed by the dotted line. Method F, resetting the integral of the rate gyroscope, and auto-nulling the rate gyroscope, is the dotted trace. (A) displays the angle as calculated through the transition. The arrows (time = 2.8, 3.8, 4.8, 5.0 and 5.2 seconds) indicate the times at which the Method F auto-nulled the rate gyroscope. (B) displays the difference between the goniometer and the accelerometer, Method E, and Method F. The breaks in this curve for Method E and Method F indicate the times at which auto-resetting of the integral occurred.*

Table 3 Comparison of accelerometer and rate gyroscope methods for calculating angle and angular velocity during the multisegment tests. The error of the angle is the root mean squared difference between the angle calculated by a goniometer and the indicated accelerometer or integrated rate gyroscope method. The error of the angular velocity is the root mean squared difference between the angular velocity calculated by a goniometer and the accelerometer or rate gyroscope

Trial	Accels. (°)	Method B (°)	Method C (°)	Method E (°)	Method F (°)	Angular velocity from rate gyroscope (°/s)	Angular velocity from accelerometers (°/s)
1	4.71	1.96	2.04	2.78	2.90	3.41	20.34
2	2.67	2.61	2.52	3.06	2.54	1.71	10.94
3	1.94	0.61	1.68	1.68	1.68	1.78	9.97
4	1.67	4.71	3.09	1.20	1.61	2.45	8.87
5	1.66	1.77	1.63	1.88	2.47	2.16	12.92
6	1.93	3.31	2.98	1.82	1.55	2.26	10.30
Mean	2.42	2.49	2.50	2.07	2.12	2.29	12.22
Std	1.18	1.41	1.41	0.70	0.58	0.62	4.19

Table 4 Comparison of accelerometer and rate gyroscope methods for calculating the angle and angular velocity on the able bodied and paraplegic individual. The average difference for the standing routine between the goniometer and the accelerometer or integrated rate gyroscope method is presented. The results are the average difference computed over the duration of the trial. The mean and standard deviation for the combined trails is displayed. The mean and (standard deviation) of the errors are listed

	Left					Right				
	Angle (°)			Angular velocity (°/s)		Angle (°)			Angular velocity (°/s)	
	Accel.	Rate gyro. (E)	Rate gyro. (F)	Accel.	Rate gyro.	Accel.	Rate gyro. (E)	Rate gyro. (F)	Accel.	Rate gyro.
Female subject	3.7 (0.7)	3.0 (1.0)	3.2 (1.5)	11 (3)	5.0 (1.2)	2.6 (1.4)	2.2 (1.0)	2.1 (1.0)	10 (2)	5.1 (1.5)
Male subject	3.1 (0.4)	2.7 (0.4)	2.8 (0.4)	14 (2)	6.3 (0.4)	3.2 (0.3)	2.9 (0.7)	2.9 (0.4)	47 (6)	10 (2.6)
Paraplegic subject						2.7 (0.6)	2.1 (0.6)	2.1 (0.7)	28 (6)	12 (3)

5.0, and 5.2 s. Auto-resetting reduced integrator error at instants 3.8, 4.8, 5.0 and 5.2, but increased the error at instant 2.8 s. The auto-nulling in method F is indicated at times 1.2, 4.6, 5.6 and 5.8 s. The drift of the null has produced a growing integration error for method C which was corrected by the auto-nulling of method F.

The results from manoeuvres numbered 1 to 6 are listed in Table 3. A statistically significant difference was not observed when comparing the accelerometers using any of the reset/nulling methods B, C, E and F. A more accurate calculation of the angle was made using the rate gyroscopes than using the accelerometers.

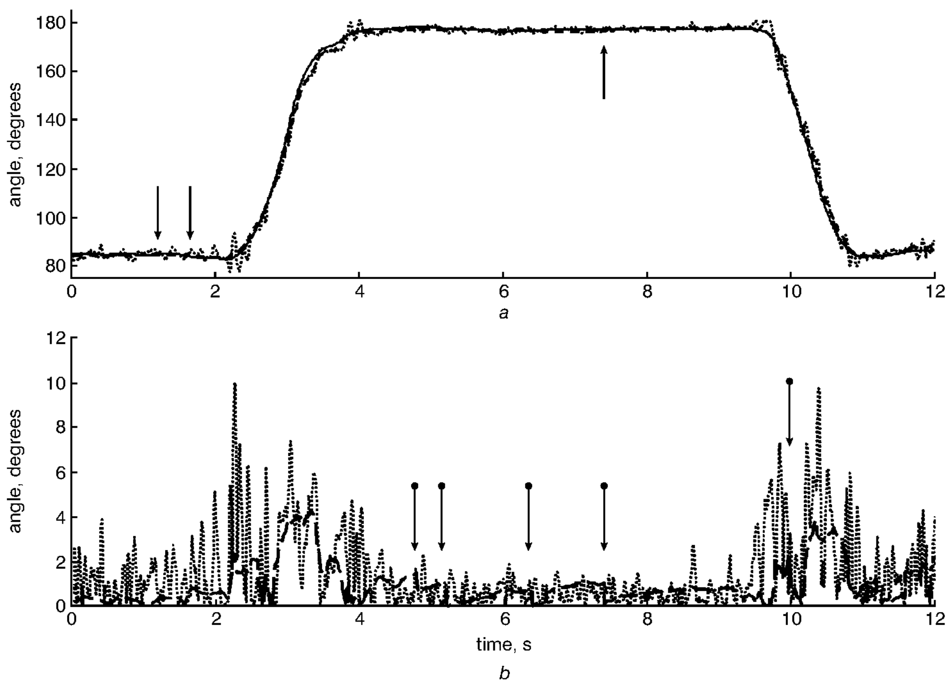

Fig. 5 *Angle calculated by goniometer, accelerometers and rate gyroscope on able-bodied volunteer. (A) displays the angle as calculated through the transition. (B) displays the difference between the goniometer and the other methods. The goniometer is the solid line. The accelerometer is the dotted line; the auto-reset auto-nulled rate gyroscope integral is the dashed line. The arrows in (A) show when the auto-nulling of the rate gyroscopes occurs. Arrows in (B) indicate the auto-reset rate gyroscope (times 4.8, 5, 6.2, 7.2 and 10 seconds).*

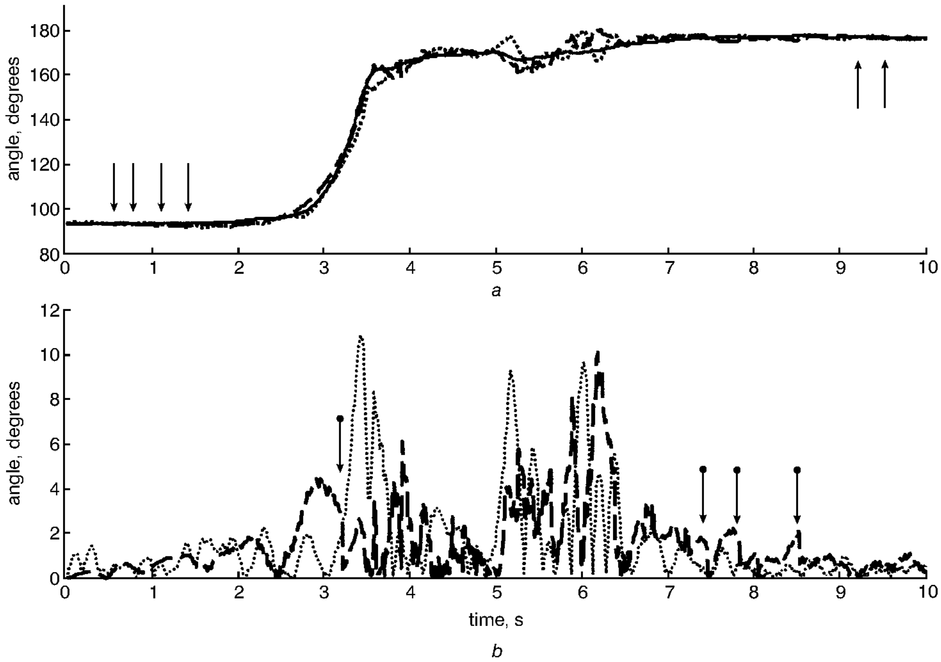

Fig. 6 *Angle calculated by goniometer, accelerometers and rate gyroscope on a paraplegic volunteer. (A) displays the angle as calculated through the transition. (B) displays the difference between the goniometer and the other methods. The goniometer is the solid line. The accelerometer is the dotted line; the auto-reset auto-nulled rate gyroscope integral is the dashed line. The arrows in (A) show when the auto-nulling of the rate gyroscopes occurs. Auto-resetting of the integrators is also displayed in (B) at times 3.2, 7.4, 7.8, and 8.2 seconds.*

The errors for trials 4 and 6 in Table 3 for methods B and C were much larger than the errors observed for methods E and F. Methods B and C were discounted from further analysis due to this increase in error.

4.2 *Sit-stand-sit trials*

Table 4 summarises the results for both the paraplegic and able bodied subjects. Fig. 5 displays a sample recording from an able bodied individual, and Fig. 6 displays the results from the paraplegic individual.

For the able bodied individuals, methods E and F, used to auto-reset the integrator and auto-null the rate gyroscopes, were able to estimate the knee angle better than the accelerometers for the entire sit–stand–sit manoeuvre. A statistical difference was not observed between the methods E and F. A better estimate of the angular velocity was made by the rate gyroscopes than by the differentiated accelerometers.

Table 5 The effect of FES on the calculation of knee angle and angular velocity during standing up as calculated by an electrogoniometer, rate gyroscope, and accelerometer. The open bandwidth and second-order Butterworth filtered values are shown for each technique. The mean and standard deviation as computed in the six trials of the paraplegic subject of the high frequency RMS are shown

	Goniometer		Rate gyroscopes integral		Accelerometer	
Angle (°)	Without FES	With FES	Without FES	With FES	Without FES	With FES
No Filter	0.870	0.607	0.023	0.102	2.746	7.105
	0.028	0.060	0.004	0.038	0.336	1.777
10 Hz	0.293	0.222	0.003	0.019	0.981	1.292
	0.052	0.021	0.000	0.007	0.109	0.289
5 Hz	0.152	0.124	0.006	0.015	0.519	0.370
	0.040	0.013	0.001	0.003	0.036	0.057
2.5 Hz	0.067	0.057	0.009	0.026	0.213	0.118
	0.021	0.001	0.003	0.008	0.055	0.016
Angular velocity (°/s)						
No Filter	132.65	91.14	1.48	19.53	401.30	904.58
	3.14	9.64	0.08	6.47	53.13	233.03
10 Hz	17.38	13.27	0.73	3.06	59.44	145.84
	2.33	1.23	0.10	1.10	5.62	34.86
5 Hz	6.35	4.83	0.45	1.15	21.51	35.85
	1.07	0.52	0.09	0.28	1.79	8.24
2.5 Hz	1.94	1.55	0.20	0.51	6.63	8.98
	0.40	0.15	0.051	0.13	0.18	2.02

For the paraplegic individual, methods E and F were more accurate than the accelerometer-derived estimates of knee angle. The rate gyroscopes provided a better estimate of the differentiated goniometer reference for knee angular velocity than the differentiated accelerometer signals.

4.3 *Analysis of high frequency residual signals due to FES*

A statistical difference was not observed between the estimates of knee angle with and without FES for the Biometrics goniometer, as indicated in Table 5. However, the power of the residual high frequency signal of both the accelerometer and rate gyroscope methods were both significantly increased by the use of FES although the level for the rate gyroscope method was still less than that for the goniometer. Low-pass filtering was found to reduce this FES-induced noise.

The use of FES did not significantly increase the RMS noise of the knee angle velocity estimate determined by the differentiated goniometer signal but did increase the residual high frequency power levels in both the accelerometer and rate gyroscope. The residual high frequency power of the rate gyroscope signal was lower than that of the goniometer. Low-pass filtering was found to reduce the RMS noise, for example, a second-order Butterworth, 3 dB cutoff at 10 Hz, reduced the RMS error of the rate gyroscopes and accelerometer methods to 3 and 146° s^{-1} respectively.

5 Discussion

In the trials on the able bodied and paraplegic individual, methods E and F provided a better estimate of angle and angular velocity than the low-pass-filtered accelerometers. This provides an initial claim that the rate gyroscope could be beneficial for real time detection of knee angle and angular velocity during standing up and sitting down. Since the rate gyroscopes signals are integrated to produce an estimate of angle, the signals did not need to be low-pass filtered, which can add delay and inaccuracy to the estimate, as seen in Table 2. The resetting algorithm appeared to contain possible errors in the integral. The auto-nulling did not demonstrate a measurable benefit in the trials, possibly due to the short period of time (20 s) in which the trials occurred. However, the auto-nulling did find a time to null the rate gyroscope both while the individual was sitting prior to each trial. This could remove the strict requirement of a calibration period prior to each trial.

Accelerometers were necessary to provide an initial estimation of the tilt of each segment, and to allow the initial angle between the clusters to be calculated. Thereafter, the accelerometers are used to determine the tilt of the segment to which the integral of the rate gyroscopes might be reset. The accuracy with which accelerometers can be used to determine their own orientation, i.e. tilt, will contribute to the overall accuracy of the rate gyroscope method. The non-linearity of the accelerometer method when compared with the goniometer was 0.5°, and was therefore a significant component of the overall error in the calculation of angles by the rate gyroscope method.

Methods E and F were accurate to within $0.7 \pm 0.2°$ in estimating the dynamic tilt (Table 1) when compared against the goniometer values. The specified accelerometer non-linearity was 0.5°, and was confirmed in a calibration. This suggests that much of the error may be due to the non-linearity of the accelerometer or the goniometer reference. Further tests using a more accurate reference angle sensor, such as a high resolution optical encoder, would be required to determine the relative contributions to the error by these sources.

For the knee angle estimates involving the segmental model, the accuracy of the rate gyroscope method F was found to be 2.1°. This was less than the errors of the trials reported on models by KATARIA and ABBAS (1998) and the computer simulations of the method proposed by LUINGE *et al.* (1999). For the tests on individuals, the accuracy of the rate gyroscope methods E and F was typically better than 4°, seen in Tables 3–5. This error is less than that reported by MIYAZAKI (1997).

The error may be due to non-linearity in the accelerometers ($0.5° \times 2$), cross-talk of the goniometer (3°), non-linearity of the goniometer (2°) (Biometrics trade literature), and the allowable static difference between accelerometer and rate gyroscope integral, indicated in eqn 5 ($1° \times 2$). The integral of the rate gyroscopes is bounded by the angle estimated from the accelerometer which in turn was compared with the goniometer. The combination of these errors indicates the maximum level of accuracy of the integral of the rate gyroscope. As the results from the tests on individuals give errors less than, methods E and F were considered to be of the order of the accuracy of estimates of knee flexion angle by a M180 goniometer.

FES increased the RMS noise of knee angle calculated by either the rate gyroscope or the accelerometer methods. However, low-pass filtering with a 3 dB cutoff at 10 Hz reduced the level to less than 0.1°. This is a higher precision than that observed using the low-pass filtered goniometer and that obtained by low-pass filtering the accelerometers.

FES also increased the RMS noise in the estimates of angular velocities. Again, low-pass filtering of the rate gyroscopes signals (3 dB at 10 Hz) reduced the RMS noise level to 3° s^{-1} which was less than that obtained from the goniometer (13° s^{-1}) or the accelerometer (145° s^{-1}).

The use of a combined accelerometer – rate gyroscope system for the measurement of knee angle and angular velocity has certain advantages in comparison to the M180 goniometer. The linkage between the two clusters is not of a fixed length, and hence strain and possible movement of the mounting due to repetitive movements should not exist, which was reported as a problem with the electrogoniometer for measuring knee angle. After the one time ± 1 g bench calibration of each sensor module, kinematic estimates of joint angle, velocity and segmental inclinations were immediately available after attaching the device and no further calibration is required, which was not the case with the goniometer.

The present restriction on placement of the clusters was that the rate gyroscopes must be mounted perpendicular to the plane of motion of which the angle was contained. Once an initial determination of the ± 1 g levels from the accelerometers were made, the devices did not require calibration, as demonstrated in method F. This means that these clusters could be placed on an individual who is sitting, and an immediate calculation of knee angle would be made. A second restriction, that the motion does not occur in a horizontal plane, could be overcome by combining this method with a non-inertial sensor such as the magnetoresistors or Hall effect sensors that would provide a reference to the earth's magnetic field.

It has been shown that the accuracy level of method E and F was better than 4°. With a goniometer, initial estimates of angle are typically approximated through a visual comparison. Induced errors are due to locating the centre of the knee joint, orientation of both the goniometer and the protractor with limb segments, and parallax. It is the authors' belief that this error is greater than the error apparent from using the combination of rate gyroscopes and accelerometers. A direct comparison of the accuracy of the combined accelerometer – rate gyroscope system and Biometrics goniometer can only be constructed by using a third measurement of knee flexion angle with accuracy an order of magnitude less than the errors of either the combined accelerometer–rate gyroscope system or the electrogoniometer. This suggests that the accuracy of the combined accelerometer–rate gyroscope system is greater than the electrogoniometer.

6 Conclusion

Based on the accuracy of the accelerometers, auto-resetting of the integral of rate gyroscopes and auto-nulling of the DC output offset provides an accurate assessment of the angle across the knee joint during sit to stand and stand to sit manoeuvres. Rate gyroscopes can provide a more accurate and precise estimation of knee angle and angular velocity than can be determined from accelerometers.

Acknowledgements—We acknowledge the support of the US Department of Health and Human Services grant # 8R3HD38494A and Neopraxis Ltd., Australia. We also thank Mr Ando Masaki of Murata Japan for the rate gyroscopes and technical information.

References

Analog Devices (1999) ADXL202 Data Sheet

ANDREWS, B. J., BARNETT, R., PHILLIPS, G., KIRKWOOD, C., DONALDSON, N., RUSHTON, D., and PERKINS, T. (1989): 'Rule base control of a hybrid FES orthosis for assisting paraplegic locomotion' *Automedica*, **11**, pp. 175–199

ANDREWS, B. J., and WILLIAMSON, R. P. (1997): 'The gyrogoniometer'. Proc. RESNA '97, pp. 262–264

Biometrics trade literature: The model M180 flexible goniometer, UK

CRAGO, P. E., CHIZECK, H. J., NEUMAN, M. R., and HAMBRECHT, F. T. (1986): 'Sensors for use with functional neuromuscular stimulation', *IEEE Trans. Biomed. Eng.*, **33**, pp. 256–268

CRAGO, P. E., LAN, N., VELTINK, P. H., ABBAS, J. J., and KANTOR, C. (1996): 'New control strategies for neuroprosthetic systems', *J. Rehab. Res. Devel.*, **33**, pp. 158–172

HEYN, R. E., MAYAGOITIA, A., NENE, V., and VELTINK, P. H. (1996): 'The kinematics of the swing phase obtained from accelerometer and gyroscope measurements', *Proc. IEEE EMBS*, pp. 857–858

KATARIA, P., and ABBAS, J. J. (1998): 'Estimating body segment orientation using a lightweight, inexpensive gyroscope'. Proc. Biomed. Eng. Soc. Conf. P, S-133

KRALJ, A., and BAJD, T. (1989): 'Functional electrical stimulation: Standing and walking after spinal cord injury' (CRC Press, CA)

LUINGE, H. J., VELTINK, P. H., and BATEN, C. T. M. (1999): 'Estimating orientation with gyroscopes and accelerometers' in VELTINK, DE VRIES, KOOPMAN and HERMANS (Eds): Proc. Int. Biomechatronics Workshop, 19–21 April, Enchede, Netherlands, pp. 214–218

MIYAZAKI, S. (1997): 'Long term unconstrained measurement of stride length and walking velocity utilizing a piezoelectric gyroscope', *IEEE Trans. Biomed. Eng.*, **44**(8), pp. 753–759

MORRIS, J. R. (1973): 'Accelerometry—a technique for the measurement of human body movements', *J. Biomech.*, **6**, pp. 729–736

MULDER, A. J., VELTINK, P. H., BOOM, H. B. K., and ZILVOLD, G. (1992): 'Low level finite state control of knee joint in paraplegic standing', *J. Biomed. Eng.*, **14**, pp. 3–8

MuRata data sheet, ENC-05EA rate gyroscope, MuRata Japan

PETROFSKY, J. S., PHILLIPS, C. A., and HEATON, H. H. (1984): 'Feedback control system for walking', *Comput. Biol. Med.*, **14**, pp. 135–149

SMIDT, G. L., DEUSINGER, R. H., ARORA, J., and ALBRIGHT, J. P. (1977): 'An automated accelerometry system for gait analysis', *J. Biomech.*, **10**, pp. 367–375

SMIDT, G. L., ARORA, J. S., and JOHNSTON, R. C. (1971): 'Accelerographic analysis of several types of walking', *Am. J. Phys. Med.*, **50**, pp. 285–300

WILLEMSEN, A. T., FRIGO, C., and BOOM, H. B. (1991): 'Lower extremity angle measurement with accelerometers—error and sensitivity analysis', *IEEE Biomed. Eng.*, **38**, pp. 1186–1189

Authors' biographies

RICHARD WILLIAMSON was born in Edmonton, AB, in 1972. He received a B.Sc. in Engineering Physics in 1994 and a PhD in 1999 from the University of Alberta. He is currently working with Second Sight, LLC. His interests include analysis of human motion, electrical nerve blocking, and restoration of vision.

BRIAN ANDREWS was trained in Cybernetics, Control Systems and Bioengineering at the Universities of Reading, Sheffield and Strathclyde respectively. He has held academic and clinical appointments in the UK, USA and Canada. He is presently a consultant at the National Spinal Injuries Centre at Stoke Mandeville Hospital with academic appointments in the Department of Cybernetics at Reading University and the Oxford Orthopaedic Engineering Centre of Oxford University. His research interests focus on applications of bioengineering and cybernetics in spinal injury.